# LCLS-II Cavity Field-Emission Tracking

Christopher Mayes
Cornell University

December 2, 2015

## 1 Introduction

The current LCLS-II design incorporates 35 cryomodules, each containing 8 CW superconducting cavities, to accelerate electrons to 4 GeV. Each cavity has the potential to field-emit electrons from an imperfection in its surface, which depending on the location and time of this emission could be further accelerated and eventually be lost in an undesirable location in the machine. These studies use the particle accelerator simulation library Bmad to map out the possibilities for such field emission [1].

## 2 Bmad model

We constructed a Bmad model of LCLS-II using the official SLAC-MAD design LCLS2scH from June 19, 2015 [2]. Initially slight deviations in the optics was observed, and found to be due to differing cavity focusing models between SLAC-MAD and Bmad. In particular, SLAC-MAD does not have transverse cavity focusing, while Bmad uses a model developed in [3]. We slightly adjusted the strengths of 5 quadruple magnets in and near the linac sections L1, L2, and L3 ($< 20\%$ levels) so that the Twiss parameters matched the design at the ends of these sections. Figure 2.1 shows the agreement. Dispersion agrees perfectly.

The injector section, while described in the SLAC-MAD model, requires detailed modeling using field maps and a space charge code such as ASTRA [4]. Using [5], we constructed an equvalent Bmad injector model that matches the 300 pC design



This material is based upon work supported by the U.S. Department of Energy,
Office of Science, under Contract No. DE-AC02-76SF00515.

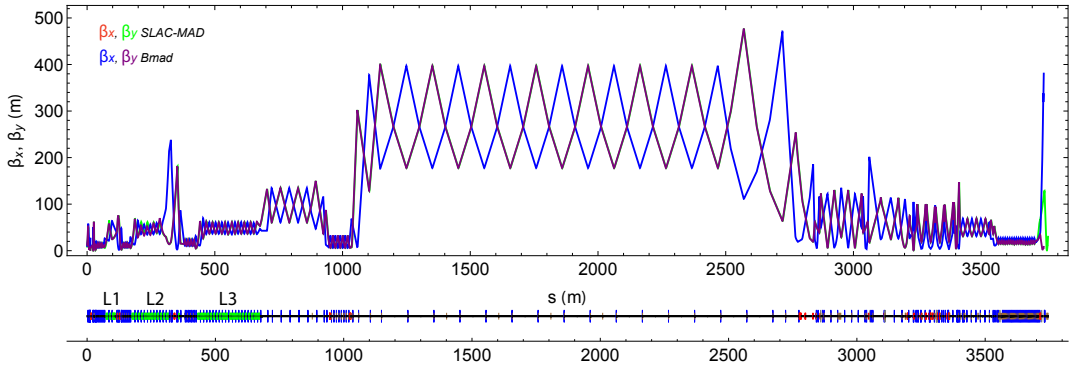


Figure 2.1: SLAC-MAD and Bmad models for LCLS2scH from June 19, 2015. Agreement is nearly perfect after quadrupoles strengths are adjusted at the ends of L1, L2, and L3 to account for the different focusing models between SLAC-MAD and Bmad. Dispersion agrees perfectly. Optics at the end are slightly off, but irrelevant for these studies.

injector. This includes 1-D and 2-D field maps for the APEX RF gun, focusing solenoids, buncher cavity, and 1.3 GHz 9-cell TESLA cavities. Figure 2.2 shows the agreement in tracking from the cathode.

Particular detail was given to the 9-cell cavity field map model, because this was also used in all linac sections. The 2-D field map was calculated using CLANS [6] and is shown in Fig. 2.3. Bmad can these fields to track particles arbitrarily in time using the Lorentz force and a Runge-Kutta integration method, as shown in Fig. 2.4. When enabled, tracking in this field map replaces the default Bmad cavity focusing model. Fortunately agreement between the two was better than 1%, so the optics did not need to be adjusted as previously. The 3.9 GHz cavities in the L1 section are modeled by simply scaling the 1.3 GHz field maps, and are not studied here for field emission.

Further detail was given to describing the vacuum chamber through all of the LCLS-II model. Bmad uses cross-sections described at particular locations, and interpolates between them to determine the wall. This is shown in Fig. 2.5 and Fig. 2.6.

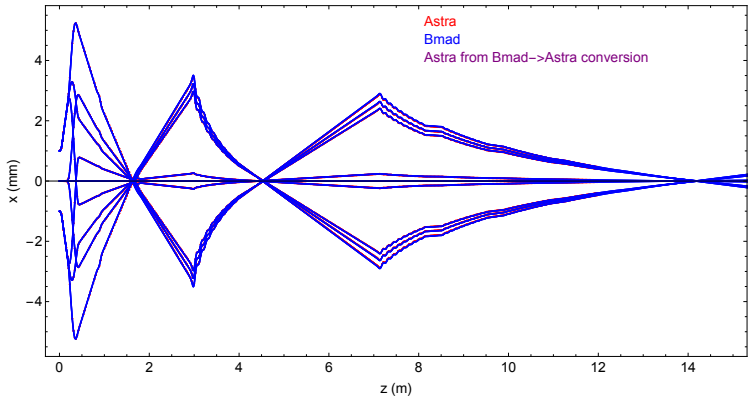


Figure 2.2: Tracking the injector model for LCLS-II using ASTRA, the equivalent Bmad model, and an ASTRA model created from the Bmad model. This is without the space charge calculation, and used only to verify that the field maps are properly aligned, scaled, and phased.

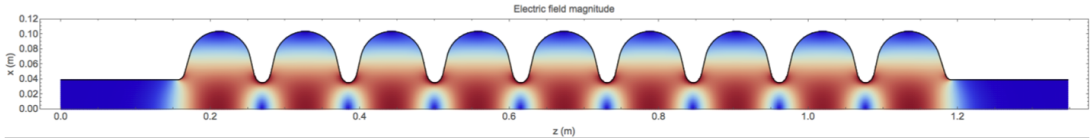


Figure 2.3: LCLS-II 1.3 GHz 9-cell cavity electric field magnitude from the Bmad field field map [6]. The cavity wall is completely described and the field is available in the full bulk of the cavity.

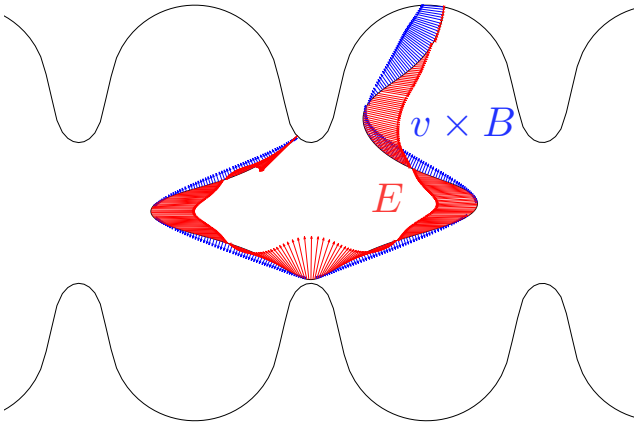


Figure 2.4: Bmad time tracking of a field emitter particle using the `time_runge_kutta` tracking method. This method allows particles to be tracked arbitrarily forwards and backwards through an entire accelerator lattice.

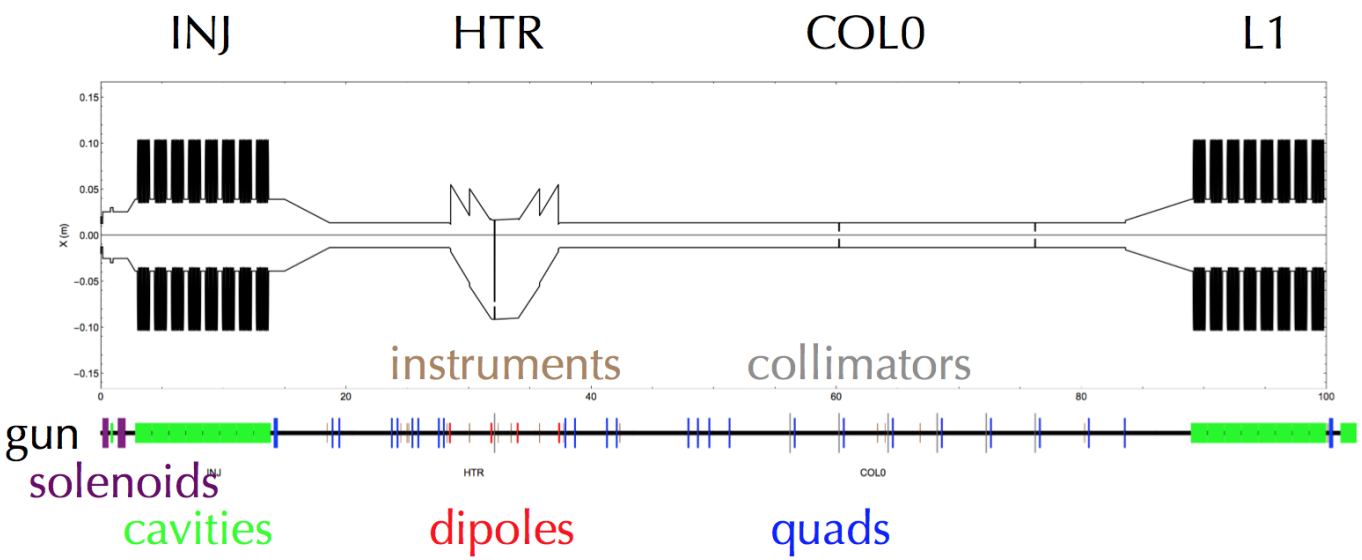


Figure 2.5: Top view of LCLS-II sections INJ (injector), HTR (laser heater), COL0 (collimators), and beginning of L1 (linac) with complete wall description in Bmad. Not shown are Mask elements in the HTR section to simulate two separate pipes. Two horizontal collimators can clearly be seen (vertical collimators cannot be seen in this view).

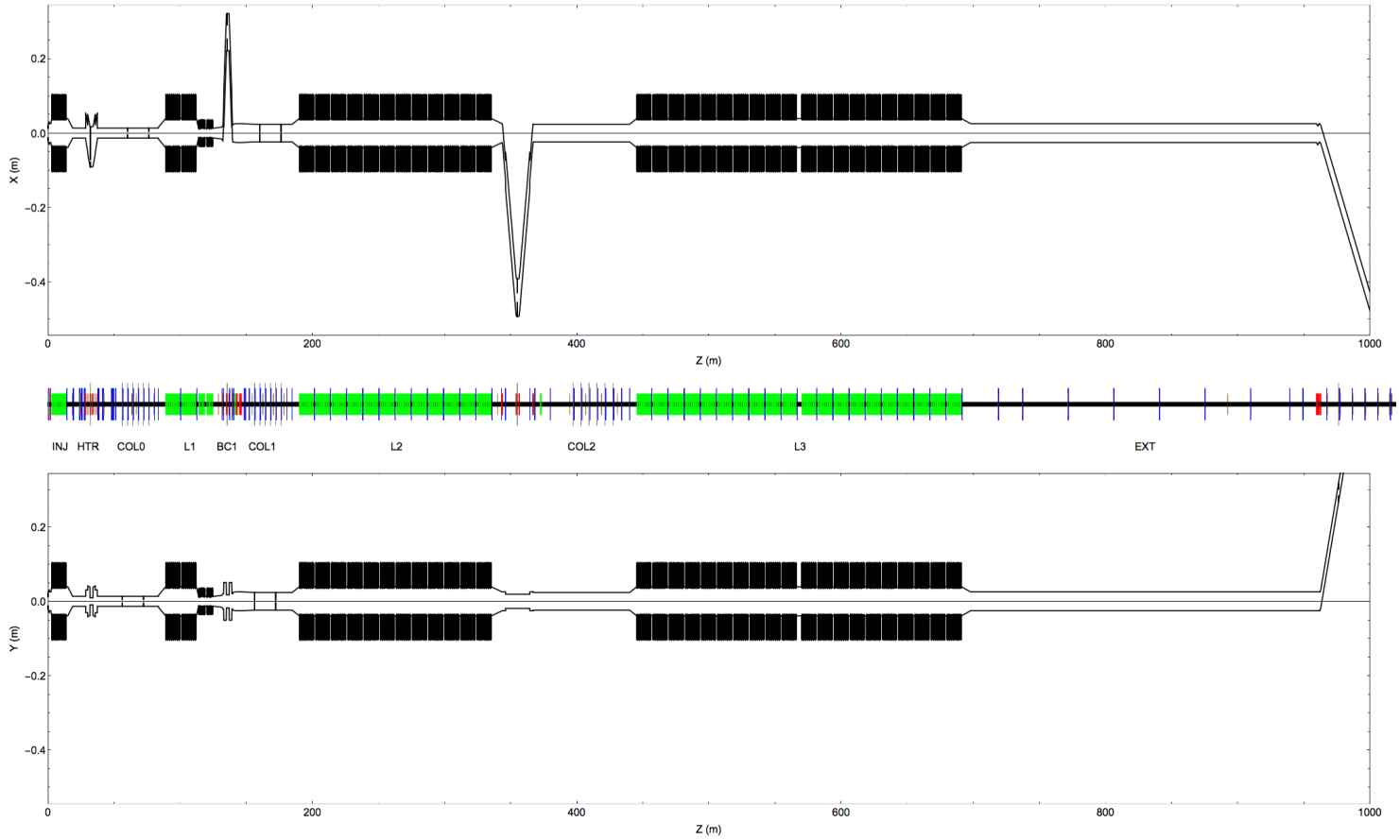


Figure 2.6: Top and Side views of the LCLS-II wall model up to the bypass line in Bmad. Collimators can clearly be seen in both the horizontal and vertical configurations. Note that the baseline design has no collimators in the COL2 section.

# 3 Field emitter tracking

The instantaneous current from Fowler-Nordheim field emission from a material surface with perpendicular electric field $E_\perp$ is given by

$$I_{\mathrm{FN}}(E_\perp) = a_0 \left(\beta_{\mathrm{FN}} E_\perp\right)^2 \exp\left(-\frac{a_1}{\beta_{\mathrm{FN}} E_\perp}\right), \tag{3.1}$$

where $\beta_{\mathrm{FN}}$ is the field enhancement factor. The factor $a_0$ sets the average current. For these simulations we use $a_1 = 5.464 \times 10^{10}\,\mathrm{V/m}$ for niobium [7]. The field enhancement factor must be determined empirically. Here we use a typical value of $\beta_{\mathrm{FN}} = 100$.

Particles from a particular field emitter are simulated using this procedure:

- Locate a position on the cavity wall.
- Sample the electric field normal $E_\perp$ at even intervals over 1 rf period.
- Create particles at this position at these times, with weights determined by Eq. (3.1).
- Only accept particles were $-eE_\perp > 0$ (accelerating outwards from the surface).
- For simplicity, normalize the weights to sum to 1.
- Track each particle until lost at the wall

Figure 3.1 shows three example field emitters and tracking of particles from them according to this procedure. One quickly discovers that only very narrow regions, called here **danger zones**, about the cavity irises can harbor field emitters that can produce particles that escape the cavity. In other words, field emitters in regions other than the danger zones will have nearly 100% losses inside of the cavity. For this reason, these studies only track particles from the danger zones.

Figure 3.3 is similar and shows that of the field emitters in the danger zones, what fraction of their current can escape the entire cryomodule. The maximum fraction in both Fig. 3.1 and Fig. 3.3 is similar, around 60%, which means that for some field emitters, if a large portion of their current escapes the cavity, some or all of this has a chance of also escaping the entire cryomodule. Furthermore, the location of the cavity in the cryomodule and the iris that the field emitter is near is not a predictor of the current fraction escaping — all irises and cavities can harbor equally 'bad' emitters.

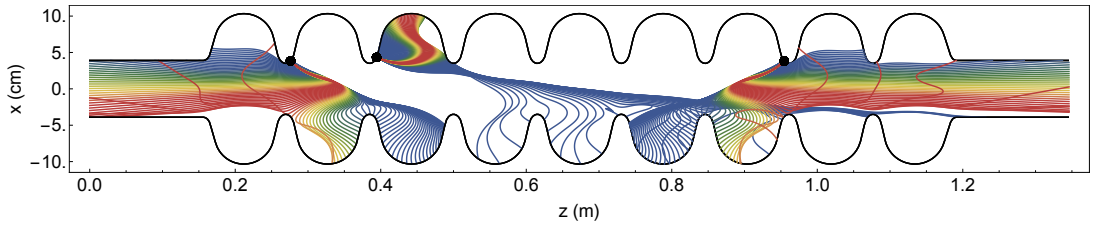


Figure 3.1: Examples of particles from field emission. Each particle is given a weight (representative current) determined by Eq. (3.1) Red represents more current, while blue represents less current.

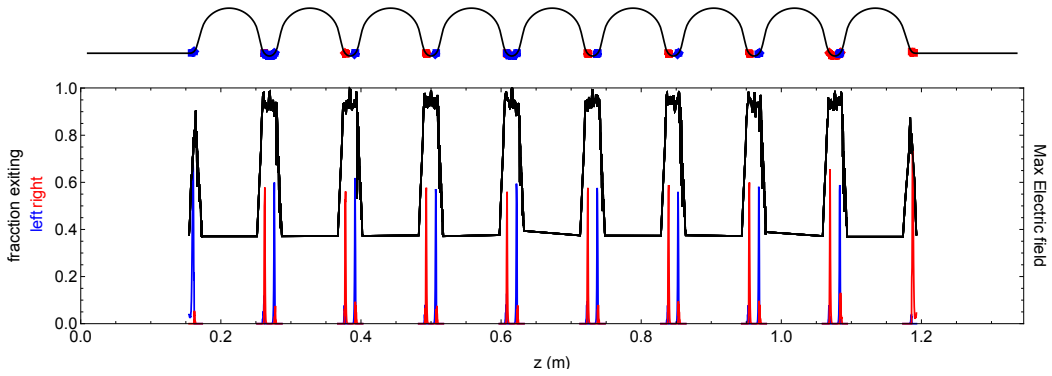


Figure 3.2: Locations of field emitters in the 9-cell cavity operating at 15 MV that can produce particles that escape the cavity, called here **danger zones**, and the fraction of their current that can escape. These regions are a few mm wide on each side of the cavity irises. Field emitters placed outside of these regions will result in losses completely within the cavity.

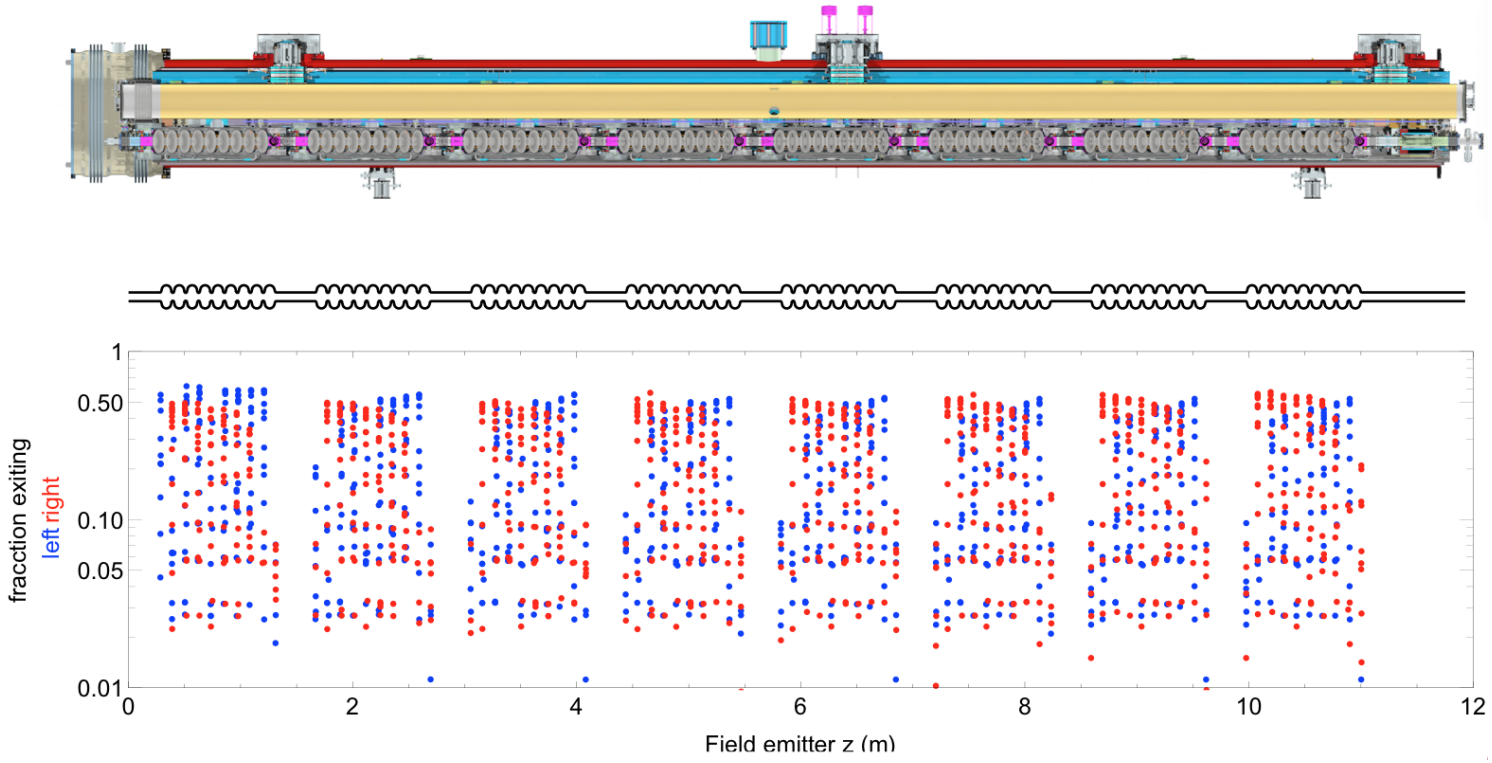


Figure 3.3: Sample field emitters only in the danger zones as in Fig. 3.2, and the fraction of their current that can escape left or right of the entire cryomodule.

# 4 Cryomodule Field Emission Scan

The current LCLS-II design specifies that no more than 10 nA of average field emission current will be allowed to escape a single cryomodule. To study the loss possibilities, we use the following procedure:

- An origin cryomodule is chosen.
- Field emitters are places only in cavity danger zones, at random azimuthal angles (here approximately 5000 emitters).
- For each emitter, particles are created with their proper Fowler-Nordheim weight and tracked through the entire accelerator until lost. (here approximately 1000 particles).
- The weights of the particles escaping the origin cryomodule are renormalized so that for each emitter, the particles lost outside the cryomodule represent 10 nA of average current.
- Power and current are tallied per element for every lost particle.

Thus about 5 million particles are tracked per cryomodule, or about 175 million particles for the entire machine. Figure 4.1 shows tracks from an example field emitter in the injector cryomodule CM01. Losses can be highly localized, as shown in Fig. 4.2.

Figure 4.3 shows the worst-case losses per element due to a single field emitter in CM01. Note that these are not tallies of different field emitters. Rather, for the power specified in the plot at an element, there is at least one field emitter in CM01 that can produce such a loss.

Figure 4.3 shows a similar tally for CM02, and interestingly shows that some particles can achieve very high energy and survive through all linac sections. However, no particle can survive past the dogleg at about 1000 m.

Figure 4.5 shows a similar tally for CM04. The possibilities for losses from this cryomodule extend backwards to BC1 and forwards up to BC2.

Plots for all 35 and complete data are available in [8].

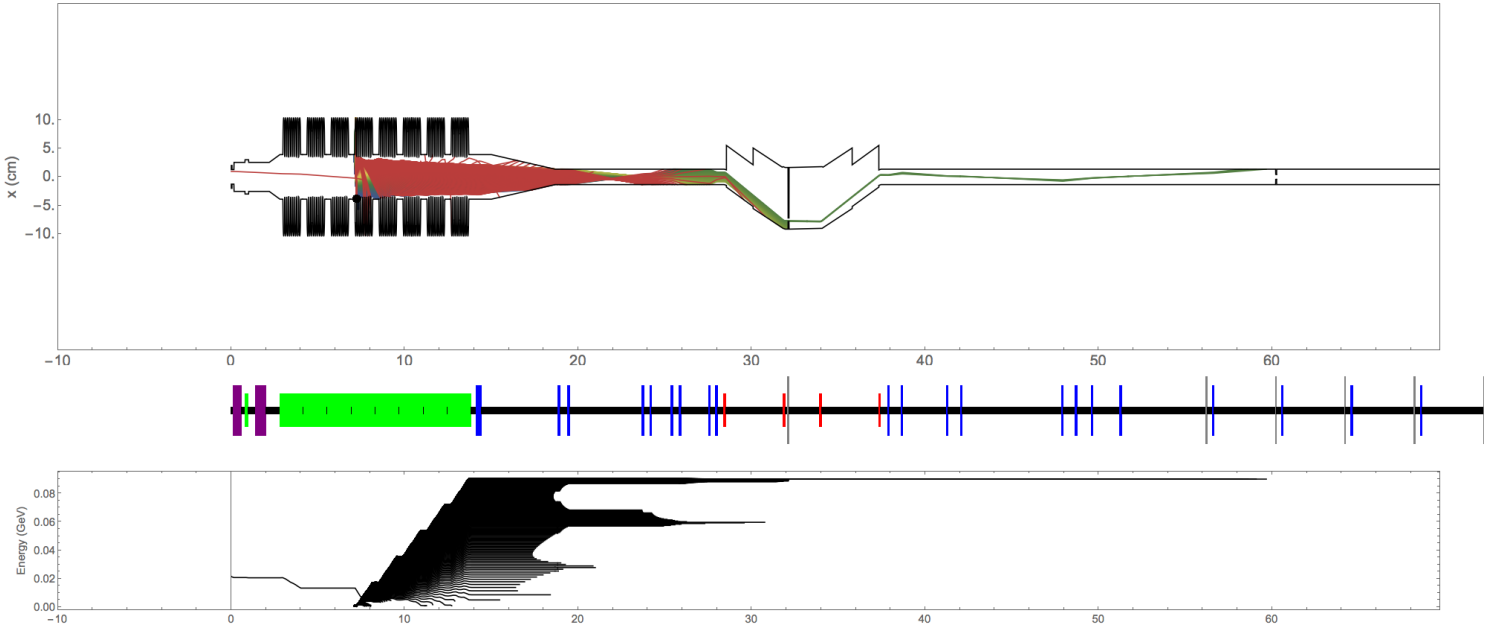


Figure 4.1: Tracks from a single field emitter in the injector cryomodule CM01. The large black dot shows the location of the emitter. One lucky particle is accelerated straight backwards into the gun. Many are lost as the vacuum chamber tapers into the HTR section, and a few survive the HTR chicane but are lost before the first collimator. The energies for all of these particles is also shown, and shows that only the highest enery particles could survive the HTR chicane.

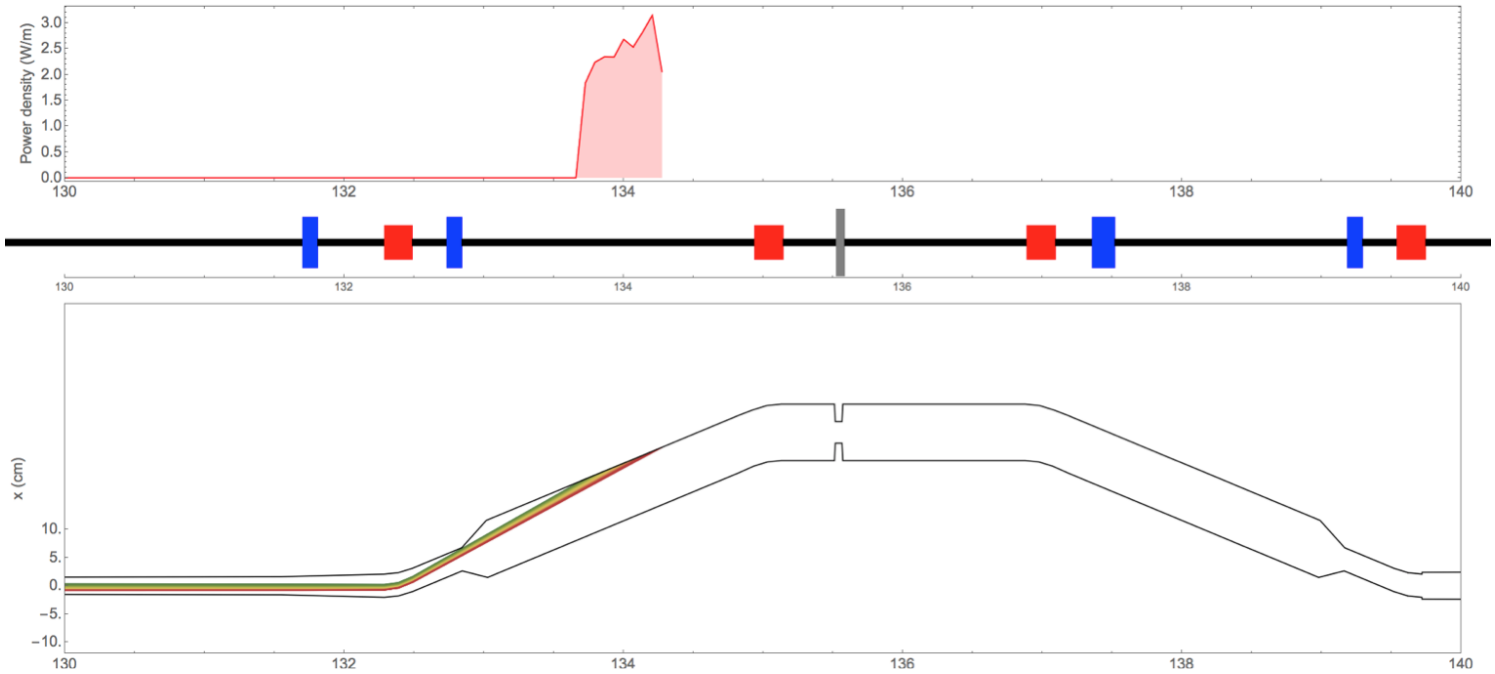


Figure 4.2: Example losses in BC2, from a single field emitter originating in CM02. The actual loss location is highly localized.

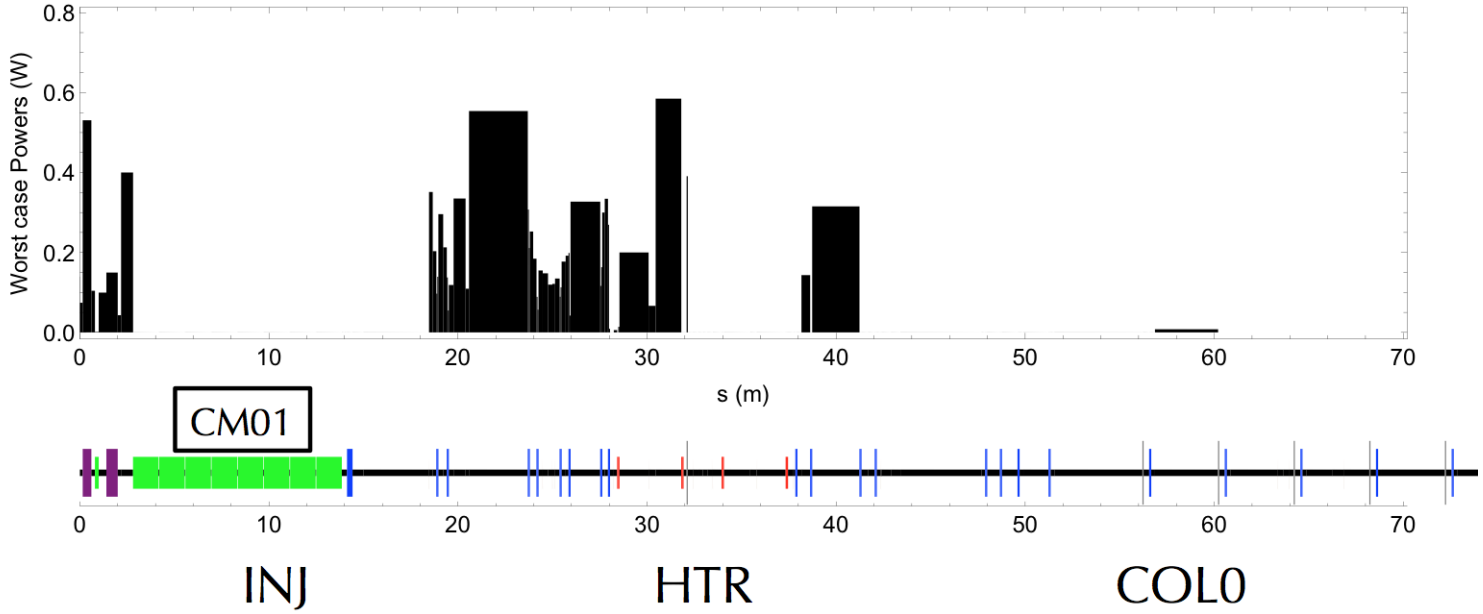


Figure 4.3: Worst-case losses in terms of power due to a single field emitter in the injector cryomodule CM01, per element. Losses inside the origin cryomodule are not shown. The plot represents the full extent of all particles tracked — no particle was lost past 70 m.

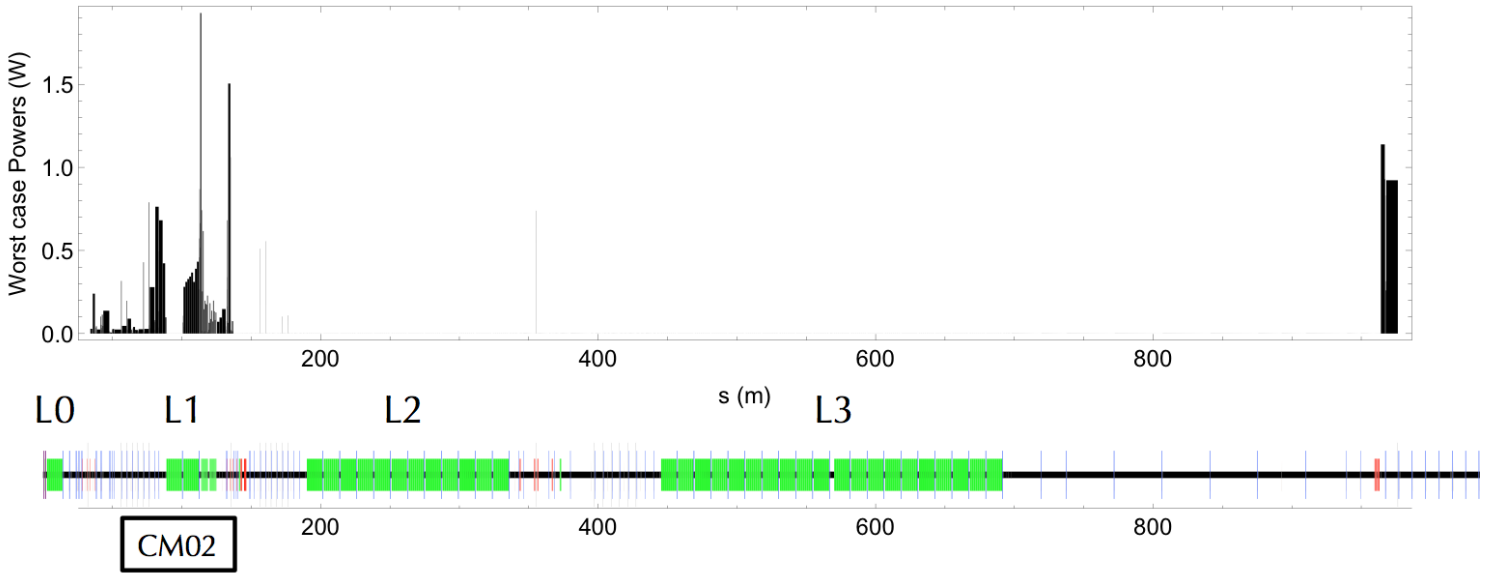


Figure 4.4: Worst cose losses in terms of power for the first cryomodule in the L1 section, CM01, similar to Fig. 4.3. Because this cryomodule is so close to the beginning of the machine, it is possible for some particles to accelerate to high energy and survive all the way up to but not past the dogleg at about 1000 m.

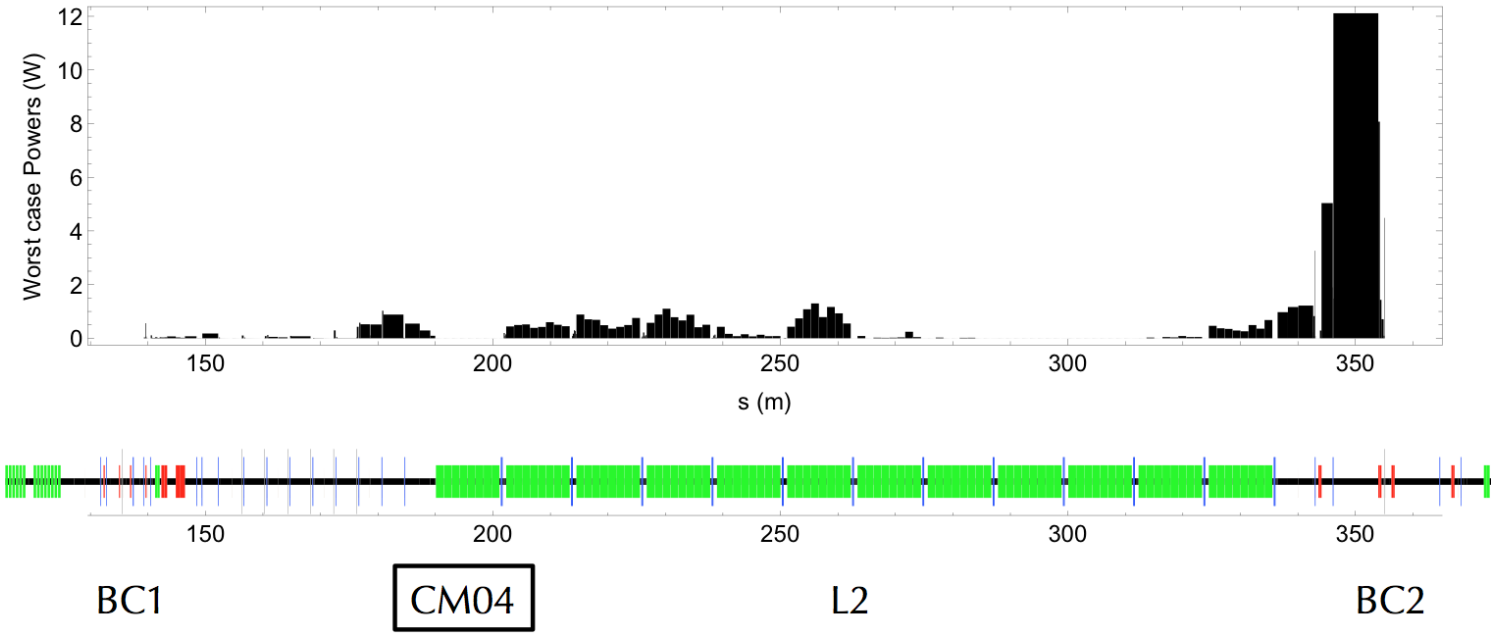


Figure 4.5: Worst cose losses in terms of power for the first cryomodule in the L2 section, CM04, similar to Fig. 4.3. Here we see that there is a chance for particles to be lost backwards. However, no particle can survive past BC1, because the magnetic field in the chicane forces the backwards particle in the opposite direction as the forward propagating beam.

# 5 Summary

Figure 5.1 is the main result of this study and shows the worst possible losses in terms of power for each element in LCLS-II. The plot shows the full extent of all possible losses, and that no field emission particle can survive the dogleg at about 1000 m. Essentially all particles created by field emission have some combination of large amplitude, wrong energy, and wrong arrival time that causes them to be lost before this point. Therefore it is impossible for the undulators in LCLS-II to be damaged by field emission.

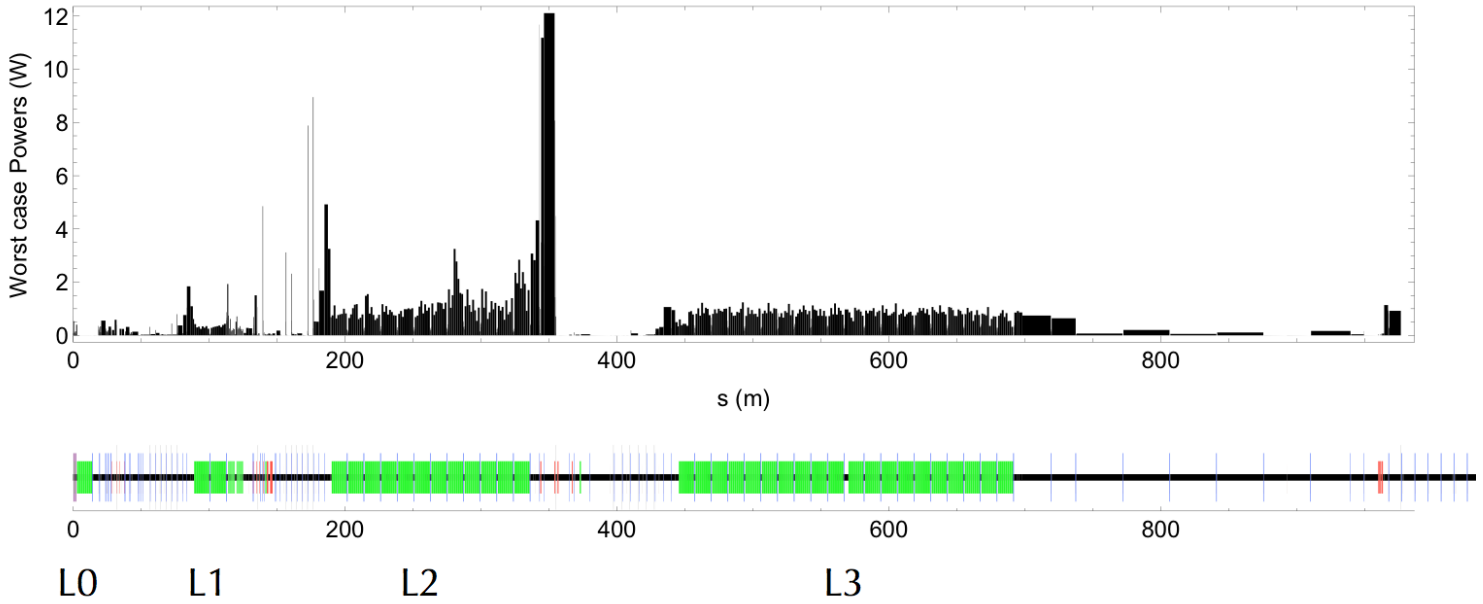


Figure 5.1: Summary of worst case losses in terms of power from all cryomodules due to a single field emitter. For each power indicated, there is at least one field emitter somewhere in the machine that can produce these losses alone. This plot does not represent a probability of such loss, only the worst case at a single element. No field emission particles can survive the dogleg at 1000 m, and thus the LCLS-II undulators cannot be damaged by field-emission from a cryomodule.

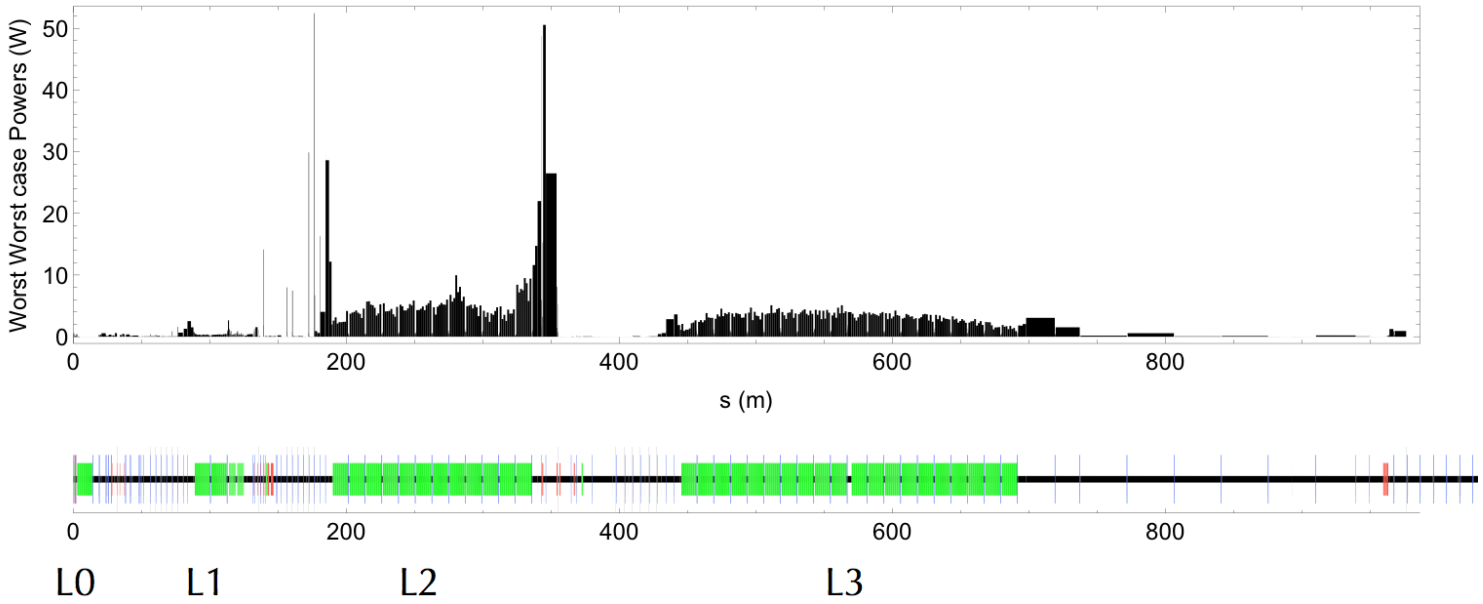


Figure 5.2: An extension of Fig. 5.1 showing the very unlikely 'worst-worst' case where, for a given element, each cryomodule has a field emitter that results in the worst losses in the element, and these losses are summed for each cryomodule. In other words, for every power indicated, there is a configuration of field emitters, one per cryomodule, that could conspire to produce this power.

# References


[1] D. Sagan, *Bmad Reference Manual*
http://www.lepp.cornell.edu/~dcs/bmad

[2] LCLS-II Lattice Description files (version 19JUN15)
http://www.slac.stanford.edu/grp/ad/model/lcls2.html

[3] J. Rosenzweig and L. Serafini, "Transverse Particle Motion in Radio?Frequency Linear Accelerators," Phys Rev E, Vol. 49, p. 1599, (1994).

[4] ASTRA - A Space-charge TRacking Algorithm,
http://www.desy.de/~mpyflo/

[5] Baseline 300 pC LCLS-II ASTRA injector model 'newbaseline300.in' courtesy of Feng Zhou (SLAC), private communication.

[6] TESLA 9-cell cavity model calculated using CLANS, courtesy of Valery Shemlin (Cornell).

[7] H. Padamsee, *RF Superconductivity*, Wiley-VCH (2009)

[8] Complete tracking data for this report:
http://www.lepp.cornell.edu/~cem52/LCLS2/data/